Low-cost board-to-board optical interconnects using molded polymer waveguide with 45 degree mirrors and inkjet-printed micro-lenses as proximity vertical coupler

Xiaohui Lin,[1] Amir Hosseini,[2] Xinyuan Dou,[1] Harish Subbaraman,[2] and Ray T. Chen[1,*]

[1]*Department of Electrical and Computer Engineering, The University of Texas at Austin, 10100 Burnet Rd, Austin, TX 78758, USA*

[2]*Omega Optics, Inc., 10306 Sausalito Dr, Austin, TX 78759, USA*

[*]*raychen@uts.cc.utexas.edu*

Abstract: We demonstrate intra- and inter-board level optical interconnects using polymer waveguides and waveguide couplers consisting of both 45 degree total internal reflection (TIR) mirrors and inkjet-printed micro-lenses. Surface normal couplers consisting of 50 μm × 50 μm waveguides with embedded 45 degree mirrors are fabricated using a nickel mold imprint. Micro-lenses, 70 μm in diameter, are inkjet-printed on top of the mirrors. We characterize the optical transmission between waveguides located on different boards in terms of insertion loss, mirror coupling loss, and free space propagation loss as a function of interconnection distance in free space. Each mirror contributes 1.88 dB loss to the system, corresponding to 65% efficiency. The printed micro-lenses improve the transmission by 2-4 dB (per coupler). Data transmission at 10 Gbps reveals that inter-board interconnects has a bit error rate (BER) of 1.1×10^{-10} and 6.2×10^{-13} without and with the micro-lenses, respectively.

©2013 Optical Society of America

OCIS codes: (200.4650) Optical interconnects; (130.5460) Polymer waveguides; (220.3630) Lenses.

References and links

1. A. K. Kodi and A. Louri, "Energy-efficient and bandwidth-reconfigurable photonic networks for high-performance computing (HPC) systems," IEEE J Sel Top Quant **17**(2), 384–395 (2011).
2. H. Cho, P. Kapur, and K. C. Saraswat, "Power comparison between high-speed electrical and optical interconnects for interchip communication," J. Lightwave Technol. **22**(9), 2021–2033 (2004).
3. G. Q. Chen, H. Chen, M. Haurylau, N. A. Nelson, D. H. Albonesi, P. M. Fauchet, and E. G. Friedman, "On-chip copper-based vs. optical interconnects: Delay uncertainty, latency, power, and bandwidth density comparative predictions," Proceedings of the IEEE 2006 International Interconnect Technology Conference, 39–41, 232 (2006).
4. L. Brusberg, M. Neitz, and H. Schroder, "Single-mode glass waveguide technology for optical inter-chip communication on board-level," Proc. SPIE **8267**, 82670M, 82670M-10 (2012).
5. J. Xue, A. Garg, B. Ciftcioglu, J. Y. Hu, S. Wang, L. Savidis, M. Jain, R. Berman, P. Liu, M. Huang, H. Wu, E. Friedman, G. Wicks, and D. Moore, "An intra-chip free-space optical interconnect," Conf Proc Int Symp C, 94–105 (2010).
6. R. Barbieri, P. Benabes, T. Bierhoff, J. J. Caswell, A. Gauthier, J. Jahns, M. Jarczynski, P. Lukowicz, J. Oksman, G. A. Russell, J. Schrage, J. F. Snowdon, O. Stübbe, G. Troster, and M. Wirz, "Design and construction of the high-speed optoelectronic memory system demonstrator," Appl. Opt. **47**(19), 3500–3512 (2008).
7. R. T. Chen, L. Lin, C. Choi, Y. J. J. Liu, B. Bihari, L. Wu, S. N. Tang, R. Wickman, B. Picor, M. K. Hibbs-Brenner, J. Bristow, and Y. S. Liu, "Fully embedded board-level guided-wave optoelectronic interconnects," Proc. IEEE **88**(6), 780–793 (2000).
8. C. C. Choi, L. Lin, Y. J. Liu, J. H. Choi, L. Wang, D. Haas, J. Magera, and R. T. Chen, "Flexible optical waveguide film fabrications and optoelectronic devices integration for fully embedded board-level optical interconnects," J. Lightwave Technol. **22**(9), 2168–2176 (2004).
9. H. P. Kuo, P. Rosenberg, R. Walmsley, S. Mathai, L. Kiyama, J. Straznicky, M. Mclaren, M. Tan, and S. Y. Wang, "Free-space optical links for board-to-board interconnects," Appl Phys A-Mater **95**(4), 955–965 (2009).
10. K. Nakama, Y. Matsuzawa, Y. Tokiwa, and O. Mikami, "Board-to-board optical plug-in interconnection using optical waveguide plug and micro hole array," IEEE Photon. Technol. Lett. **23**(24), 1881–1883 (2011).

#176924 - $15.00 USD Received 26 Sep 2012; revised 14 Dec 2012; accepted 15 Dec 2012; published 2 Jan 2013

11. R. Dangel, C. Berger, R. Beyeler, L. Dellmann, M. Gmur, R. Hamelin, F. Horst, T. Lamprecht, T. Morf, S. Oggioni, M. Spreafico, and B. J. Offrein, "Polymer-waveguide-based board-level optical interconnect technology for datacom applications," IEEE Trans. Adv. Packag. **31**(4), 759–767 (2008).
12. J. Van Erps, N. Hendrickx, C. Debaes, P. Van Daele, and H. Thienpont, "Discrete out-of-plane coupling components for printed circuit board-level optical interconnections," IEEE Photon. Technol. Lett. **19**(21), 1753–1755 (2007).
13. J. J. Yang, A. S. Flores, and M. R. Wang, "Array waveguide evanescent ribbon coupler for card-to-backplane optical interconnects," Opt. Lett. **32**(1), 14–16 (2007).
14. A. Flores, S. Y. Song, J. J. Yang, Z. Q. Liu, and M. R. Wang, "High-speed optical interconnect coupler based on soft lithography ribbons," J. Lightwave Technol. **26**(13), 1956–1963 (2008).
15. P. Pepeljugoski and D. Kuchta, "Jitter performance of short length optical interconnects for rack-to-rack applications," Ofc: 2009 Conference on Optical Fiber Communication, Vols 1–5, 1797–1799 (2009).
16. J. Sakai, A. Noda, M. Yamagishi, T. Ohtsuka, K. Sunaga, H. Sugita, H. Takahashi, M. Oda, H. Ono, K. Yashiki, and H. Kouta, "20Gbps/ch optical interconnection between SERDES devices over distances from Chip-to-chip to rack-to-rack," 2008 34th European Conference on Optical Communication (ECOC) (2008).
17. J. W. Goodman, F. J. Leonberger, S. Y. Kung, and R. A. Athale, "Optical interconnections for Vlsi systems," Proc. IEEE **72**(7), 850–866 (1984).
18. D. A. B. Miller, "Optical interconnects to silicon," IEEE J Sel Top Quant **6**(6), 1312–1317 (2000).
19. Y. Li, T. Wang, and R. A. Linke, "VCSEL-array-based angle-multiplexed optoelectronic crossbar interconnects," Appl. Opt. **35**(8), 1282–1295 (1996).
20. D. V. Plant, B. Robertson, H. S. Hinton, M. H. Ayliffe, G. C. Boisset, W. Hsiao, D. Kabal, N. H. Kim, Y. S. Liu, M. R. Otazo, D. Pavlasek, A. Z. Shang, J. Simmons, K. Song, D. A. Thompson, and W. M. Robertson, "4 x 4 vertical-cavity surface-emitting laser (VCSEL) and metal-semiconductor-metal (MSM) optical backplane demonstrator system," Appl. Opt. **35**(32), 6365–6368 (1996).
21. E. M. Strzelecka, D. A. Louderback, B. J. Thibeault, G. B. Thompson, K. Bertilsson, and L. A. Coldren, "Parallel free-space optical interconnect based on arrays of vertical-cavity lasers and detectors with monolithic microlenses," Appl. Opt. **37**(14), 2811–2821 (1998).
22. E. M. Strzelecka, G. D. Robinson, L. A. Coldren, and E. L. Hu, "Fabrication of refractive microlenses in semiconductors by mask shape transfer in reactive ion etching," Microelectron. Eng. **35**(1-4), 385–388 (1997).
23. J. Chou, K. Yu, D. Horsley, R. Walmsley, M. Tan, S. Y. Wang, and M. Wu, "Characterization of a MEMS based optical system for free-space board-to-board optical interconnects," 2010 Conference on Optical Fiber Communication Ofc Collocated National Fiber Optic Engineers Conference Ofc-Nfoec (2010).
24. J. Chou, K. Yu, D. Horsley, B. Yoxall, S. Mathai, M. R. T. Tan, S. Y. Wang, and M. C. Wu, "Robust free space board-to-board optical interconnect with closed loop MEMS tracking," Appl Phys A-Mater **95**(4), 973–982 (2009).
25. T. Sakano, T. Matsumoto, and K. Noguchi, "Three-dimensional board-to-board free-space optical interconnects and their application to the prototype multiprocessor system: Cosine-III," Appl. Opt. **34**(11), 1815–1822 (1995).
26. F. Wu, L. Vj, M. S. Islam, D. A. Horsley, R. G. Walmsley, S. Mathai, D. Houng, M. R. T. Tan, and S.-Y. Wang, "Integrated receiver architectures for board-to-board free-space optical interconnects," Appl Phys A-Mater **95**(4), 1079–1088 (2009).
27. C. J. Henderson, B. Robertson, D. G. Leyva, T. D. Wilkinson, D. C. O'Brien, and G. Faulkner, "Control of a free-space adaptive optical interconnect using a liquid-crystal spatial light modulator for beam steering," Opt. Eng. **44**(7), 075401 (2005).
28. J. H. Choi, L. Wang, H. Bi, and R. T. Chen, "Effects of thermal-via structures on thin-film VCSELs for fully embedded board-level optical interconnection system," IEEE J Sel Top Quant **12**(5), 1060–1065 (2006).
29. Y. J. Liu, L. Lin, C. Choi, B. Bihari, and R. T. Chen, "Optoelectronic integration of polymer waveguide array and metal-semiconductor-metal photodetector through micromirror couplers," IEEE Photon. Technol. Lett. **13**(4), 355–357 (2001).
30. L. Schares, J. A. Kash, F. E. Doany, C. L. Schow, C. Schuster, D. M. Kuchta, P. K. Pepeljugoski, J. M. Trewhella, C. W. Baks, R. A. John, L. Shan, Y. H. Kwark, R. A. Budd, P. Chiniwalla, F. R. Libsch, J. Rosner, C. K. Tsang, C. S. Patel, J. D. Schaub, R. Dangel, F. Horst, B. J. Offrein, D. Kucharski, D. Guckenberger, S. Hegde, H. Nyikal, C. K. Lin, A. Tandon, G. R. Trott, M. Nystrom, D. P. Bour, M. R. T. Tan, and D. W. Dolfi, "Terabus: Terabit/second-class card-level optical interconnect technologies," IEEE J Sel Top Quant **12**(5), 1032–1044 (2006).
31. L. Wang, X. L. Wang, W. Jiang, J. H. Choi, H. Bi, and R. Chen, "45 degrees polymer-based total internal reflection coupling mirrors for fully embedded intraboard guided wave optical interconnects," Appl. Phys. Lett. **87**, ••• (2005).
32. C. T. Chen, H. L. Hsiao, C. C. Chang, P. K. Shen, G. F. Lu, Y. C. Lee, S. F. Chang, Y. S. Lin, and M. L. Wu, "4 channels x 10-Gbps optoelectronic transceiver based on silicon optical bench technology," Proc. SPIE **8267**, (2012).
33. B. Van Hoe, E. Bosman, J. Missinne, S. Kalathimekkad, G. Van Steenberge, and P. Van Daele, "Novel coupling and packaging approaches for optical interconnects," Proc. SPIE **8267**, 82670T, 82670T-11 (2012).
34. G. M. Jiang, S. Baig, and M. R. Wang, "Soft lithography fabricated polymer waveguides with 45 degrees inclined mirrors for card-to-backplane optical interconnects," Proc. SPIE **8267**, ••• (2012).
35. J. Inoue, T. Ogura, K. Kintaka, K. Nishio, Y. Awatsuji, and S. Ura, "Fabrication of embedded 45-degree micromirror using liquid-immersion exposure for single-mode optical waveguides," J. Lightwave Technol. **30**(11), 1563–1568 (2012).

#176924 - $15.00 USD Received 26 Sep 2012; revised 14 Dec 2012; accepted 15 Dec 2012; published 2 Jan 2013
(C) 2013 OSA

36. C. C. Chang, P. K. Shen, C. T. Chen, H. L. Hsiao, Y. C. Chang, Y. C. Lee, and M. L. Wu, "Transmitting part of optical interconnect module with three-dimensional optical path," Proc. SPIE **8267**, ••• (2012).
37. A. L. Glebov, M. G. Lee, and K. Yokouchi, "Integration technologies for pluggable backplane optical interconnect systems," Opt. Eng. **46**(1), 015403 (2007).
38. B. Ciftcioglu, G. Jing, R. Berman, M. Jain, D. Moore, G. Wicks, M. Huang, E. G. Friedman, and W. Hui, "Recent progress on 3-D integrated intra-chip free-space optical interconnect," in *Optical Interconnects Conference, 2012 IEEE*, 2012), 56–57.
39. B. Ciftcioglu, R. Berman, S. Wang, J. Y. Hu, I. Savidis, M. Jain, D. Moore, M. Huang, E. G. Friedman, G. Wicks, and H. Wu, "3-D integrated heterogeneous intra-chip free-space optical interconnect," Opt. Express **20**(4), 4331–4345 (2012).
40. X. L. Wang, W. Jiang, L. Wang, H. Bi, and R. T. Chen, "Fully embedded board-level optical interconnects from waveguide fabrication to device integration," J. Lightwave Technol. **26**(2), 243–250 (2008).
41. X. Y. Dou, X. L. Wang, H. Y. Huang, X. H. Lin, D. Ding, D. Z. Pan, and R. T. Chen, "Polymeric waveguides with embedded micro-mirrors formed by Metallic Hard Mold," Opt. Express **18**(1), 378–385 (2010).
42. X. Lin, A. Hosseini, A. X. Wang, and R. T. Chen, "Reduced surface roughness with improved imprinting technique for polymer optical components," in *Photonics Conference (IPC), 2012 IEEE*, 2012), 280–281.
43. C. H. Tien, C. H. Hung, and T. H. Yu, "Microlens arrays by direct-writing inkjet print for LCD backlighting applications," J Disp Technol **5**(5), 147–151 (2009).
44. J. Y. Kim, N. B. Brauer, V. Fakhfouri, D. L. Boiko, E. Charbon, G. Grutzner, and J. Brugger, "Hybrid polymer microlens arrays with high numerical apertures fabricated using simple ink-jet printing technique," Opt. Mater. Express **1**(2), 259–269 (2011).
45. V. Fakhfouri, N. Cantale, G. Mermoud, J. Y. Kim, D. Boiko, E. Charbon, A. Martinoli, and J. Brugger, "Inkjet printing of SU-8 for polymer-based MEMS a case study for microlenses," Mems 2008: 21st IEEE International Conference on Micro Electro Mechanical Systems, Technical Digest, 407–410 (2008).
46. B. Xu, W. Yu, M. Yao, M. R. Pepper, and J. H. Freeland-Graves, "Three-dimensional surface imaging system for assessing human obesity," Opt. Eng. **48**(10), a156427 (2009).
47. I. A. Grimaldi, A. D. Del Mauro, F. Loffredo, G. Nenna, F. Villani, and C. Minarini, "Microlens array manufactured by inkjet printing: study of the effects of the solvent and the polymer concentration on the microstructure shape," Optical Measurement Systems for Industrial Inspection Vii **8082**(2011).
48. A. Voigt, U. Ostrzinski, K. Pfeiffer, J. Y. Kim, V. Fakhfouri, J. Brugger, and G. Gruetzner, "New inks for the direct drop-on-demand fabrication of polymer lenses," Microelectron. Eng. **88**(8), 2174–2179 (2011).
49. K. H. Jeong and L. P. Lee, "A new method of increasing numerical aperture of microlens for biophotonic MEMS," Eng Med Biol Soc Ann, 380–383 (2002).
50. F. Morichetti, A. Melloni, C. Ferrari, and M. Martinelli, "Error-free continuously-tunable delay at 10 Gbit/s in a reconfigurable on-chip delay-line," Opt. Express **16**(12), 8395–8405 (2008).
51. H. C. Hansen Mulvad, L. K. Oxenløwe, M. Galili, A. T. Clausen, L. Grüner-Nielsen, and P. Jeppesen "1.28 Tbit/s single-polarisation serial OOK optical data generation and demultiplexing," Electron. Lett. **45**(5), 280–U260 (2009).

1. Introduction

The increasing clock speed in current high performance computing system imposes an increasing demand on data transfer rates with increasingly stringent requirements for latency and power consumption per bit [1]. The current copper based electrical interconnects face serious challenges to meet such demands [2, 3]. Optical communication systems are emerging as alternative approaches at several levels including chip-to-chip [4–6], intra-board [7, 8], board-to-board [9–12], card-to-backplane [13, 14] and rack-to-rack interconnects [15, 16]. Optical interconnects consisting of arrays of Vertical Cavity Surface-Emitting Lasers (VCSELs) and Photo-detectors (PDs) have been shown to be superior to copper based electrical interconnects in terms of cost, power, and bandwidth [17, 18].

Parallel data transmission through optical means between boards has been demonstrated with complex packaging involving discrete micro and macro lenses and stage-alignment tools [19, 20]. Free-space optical interconnects between VCSELs and PDs placed on separate boards have been demonstrated in which fixed integrated micro-lens arrays [21, 22] or MEMS controlled lens arrays were used to lower optical loss by reducing the beam divergence [23–27]. In this paper, intra-board and inter-board optical interconnects are demonstrated. Intra-board interconnects are realized using 50 μm × 50 μm polymer waveguide. Inter-board coupling scheme is realized by 45 degree mirrors and integrated inkjet-printed micro-lenses. It provides free-space optical interconnects between waveguides located on different boards. The 45 degree mirrors, which are fabricated through a 3D molding technique, enable vertical coupling of guided-wave with high efficiency. Inkjet-

#176924 - $15.00 USD Received 26 Sep 2012; revised 14 Dec 2012; accepted 15 Dec 2012; published 2 Jan 2013
(C) 2013 OSA

printed micro-lenses are shown to significantly decrease the divergence and increase the quality of collimation of the vertical beam.

45 degree mirror couplers were previously used for integrating VCSELs and PDs in one of PCB board layers by Choi [28], Liu [29], Schares [30] and Wang [31]. 6.0 dB (0.5 mm transmission line) and 6.4 dB (80 mm waveguide) coupling losses, including two 45 degree mirrors, respectively were reported by Chen [32] and Van Hoe [33]. More recently, Jiang [34] and Inoue [35] reported 1.74 dB and 2.3 dB coupling loss, respectively for one 45 degree mirror. Chang etc [36]. reported insertion loss through two mirrors, over 0.5mm distance in bulk silicon and waveguide to be 8.0 dB. The lowest loss was reported in ref [37], where a mechanical saw with a 90-deg V-shaped diamond blade was used to make 45 degree mirror with 0.5 dB loss. Besides, some researchers utilized precisely positioned external coupling module [12] or external lens to maximize the coupling efficiency [38, 39]. However, such external components usually have large footprint and are not suitable for system integration.

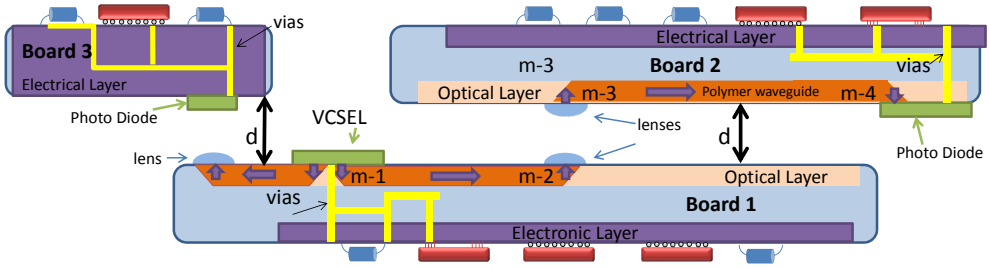

Fig. 1. Inter- and intra-board optical interconnects with polymer waveguides and 45o couplers with ink-jet printed micro-lenses.

In this work, we fabricate embedded total internal reflection (TIR) mirrors in a single-step molding process using nickel mold. Similar process has been reported by Wang [40], but using silicon mold. Nickel molds are advantageous over silicon mold because they can be formed by electroplating method to reach 50μm height while etching silicon to the same depth is rather challenging. The embedded mirrors together with the inkjet-printed micro-lenses on top serve as proximity couplers for board-to-board free-space optical interconnects between two molded waveguides on separate boards. A schematic of the presented board-to-board optical communication scheme is shown in Fig. 1. The VCSEL and PD can be controlled by signals transmitted through vias from the electric layer onto the other side of the board. The boards are positioned back-to-back to enable the data transfer via the optical couplers. This technique can be used to couple light between waveguides, i.e, light from a VCSEL into an input waveguide, or light from an output waveguide into a PD, as shown in Fig. 1. We investigate the optical transmission quality in setups using two mirrors and four mirrors in the optical path. Losses as a function of different board-to-board separations are also measured. In order to investigate the effects of inkjet-printed micro-lens, insertion losses with and without the micro-lenses are compared.

2. Mirror coupler fabrication process

We fabricate polymer waveguides with embedded 45 degree mirrors using molding method on a flexible substrate and attach it to the silicon chip. The fabrication is composed of four main steps as illustrated in Fig. 2: (a) SU8 pre-mold fabrication, (b) nickel metal mold by electroplating, (c) molding process, and (d) waveguide fabrication. SEM pictures (for steps a, b and c) and microscopic pictures (for step d) are also shown.

#176924 - $15.00 USD Received 26 Sep 2012; revised 14 Dec 2012; accepted 15 Dec 2012; published 2 Jan 2013
(C) 2013 OSA

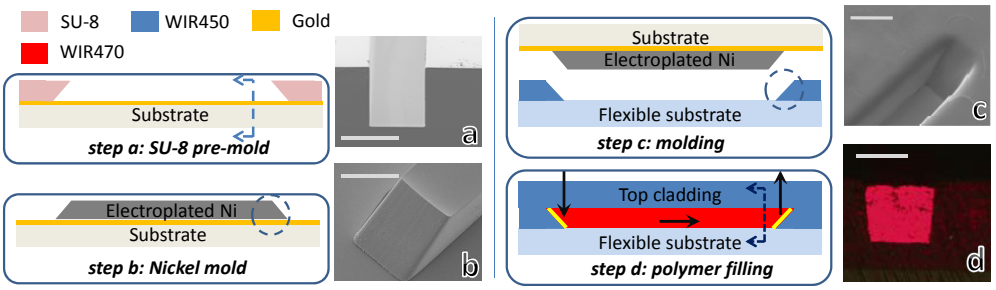

Fig. 2. fabrication process for molded channel waveguide with 45 degree embedded mirror coupler. The scale bar represents 50μm length.

2.1 SU8 pre-mold fabrication

The 1st step (step a) is making SU8 pre-mold with 45 degree mirrors on both sides. The pre-mold is used as a template for the nickel hard mold and its fabrication quality is of great importance for all the following steps. First, a thin layer of 5 nm/50 nm Ti/Au layer is coated by evaporation and serves as a seed layer for electroplating nickel performed in step b as shown in Fig. 2. Following this, a 50 μm thick SU-8 layer is deposited on the seed layer and patterned by immersed tilted exposure to form the 45° slants. The detailed description can be found in [41].

2.2 Nickel hard mold electroplating

In this step nickel is electroplated on the SU8 template. Compared to the evaporation/lift-off methods, electroplating is featured by its high deposition rate, and makes it possible to deposit 50μm in less than 7 hours. We use a Ni electroplating kit that is commercially available from Caswell Inc. The pre-buried Ti/Au layer serves as the seed layer for electroplating. In order to achieve the required adhesion between the seed layer and the nickel layer, the electro-plating current density is initially kept low at 1 mA/cm^2 for 5 minutes. Then, the current density is raised to 10 mA/cm^2 to achieve a deposition rate of 120 nm/min. At the end, a low current density 1 mA/cm^2 is applied for 5 minutes to improve film quality. Next, the SU-8 resist is removed by Remover PG to release the nickel mold. The cross linked SU-8 resist is hard to be removed by any solvent therefore, it is important to have a release layer underneath the SU-8 layer, for example Omnicoat, to help peel off the cross linked SU-8 completely.

2.3 Imprinting the channel on the bottom cladding

A 200μm thick flexible TEONEX thin film (from DuPont Teijin Films Inc.) serves as the substrate. The bottom cladding material WIR30-450 (n = 1.45@850 nm) is spin-coated on the substrate together with an adhesion promoter in-between, followed by Ultraviolet (UV) light curing. To ensure the mold can be effectively detached from the substrate during the molding process, AZ5209 photo resist is spin-coated on nickel hard mold as the release layer. At the same time, this release layer also helps reducing the surface roughness of mold. Atomic force microscopy (AFM) is used to evaluate the surface condition as shown in Fig. 3(a). The scan results reveal that the surface roughness of the mold is reduced from 70nm [Fig. 3(b)] to 2~3nm [Fig. 3(c)] by resist coating. After molding, the polymer is UV cured. Next, the de-molding process is completed in acetone, which dissolves the photo resist in-between the mold and device. The molded surface roughness is less than 5nm as reported before [42].

#176924 - $15.00 USD Received 26 Sep 2012; revised 14 Dec 2012; accepted 15 Dec 2012; published 2 Jan 2013
(C) 2013 OSA

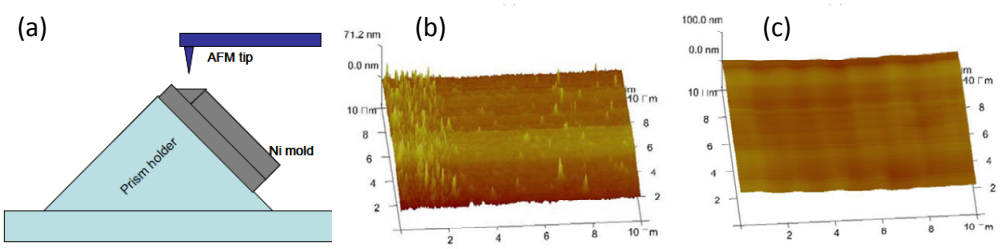

Fig. 3. (a) AFM scanning the 45 degree slope for surface roughness; (b) surface of electroplated Ni; (c) after coating releasing layer

2.4 Waveguide layer and embedded mirror formation

The molded bottom cladding layer is mounted on the evaporation chamber and 200 nm of gold is coated onto the slope region using a shadow mask. Gold coating helps to enhance the reflectivity of the mirror, which in turn increases the coupling efficiency. The imprinted trenches are filled with the core material WIR30-470 (n = 1.47@850 nm). Next, the core material is UV cured for 12 min followed by coating of the top cladding.

3. Micro-Lens fabrication process

In the present experiment, the optical signal receiving area is about the same size as the output end. Therefore, the light collected is very limited due to divergence and separation between two boards. Inserting a micro-lens in the optical path helps in reducing the divergent angle of output light from the 45 degree mirrors so that more signal can be collected. The micro-lenses have been fabricated based on photoresist melt-and-reflow technique [6, 39]. In this work, the micro-lenses are directly ink-jet printed over the 45 degree mirrors, similar to the method reported in [43]. In our experiment, we use diluted glycerol (glycerol:BPS = 3:7 by volume) to form the micro-lens with index of 1.46556 at 850 nm wavelength. The ink-jet printer used in this work is a Fujifilm Dimatix Materials Printer (DMP-2800). It utilizes a piezoelectric printing cartridge (DMC-11610), which dispenses a nominal volume of 10pL each cycle for one nozzle. By specifying the desired printing position, the micro-lens can be placed above the targeted 45 mirror coupler with good accuracy. Figure 4(a) and Fig. 4(b) show the top view of the mirror before and after inkjet-printing the micro-lens. A contact angle goniometer is used to take the profile of the droplet, as shown in Fig. 4(c).

The lens profile, which determines the focal length, can be adjusted by varying the viscosity of the printed material or surface properties of the substrate. Also, UV curable material can be adopted and cured to permanently fix the shape of the micro-lens [43]. Different focal lengths have been reported, for example, 48 μm [44], 55-153 μm [45], a few hundred microns [23, 46–48], or in millimeter range [9], with different materials and lens profiles. Currently, the printed droplets in this work are 70μm in diameter with 100-150 μm focal lengths estimated using the relations in [49]. The focal length can be controlled by the combination of surface properties, material viscosity and ink volumes. We are still investigating the effects of different refractive index, size, curvature and contact angle of the inkjet-printed lenses. By fine tuning the lens profile, optimized focal length can be achieved to make sure that light collected at the receiving end is maximized.

#176924 - $15.00 USD Received 26 Sep 2012; revised 14 Dec 2012; accepted 15 Dec 2012; published 2 Jan 2013
(C) 2013 OSA

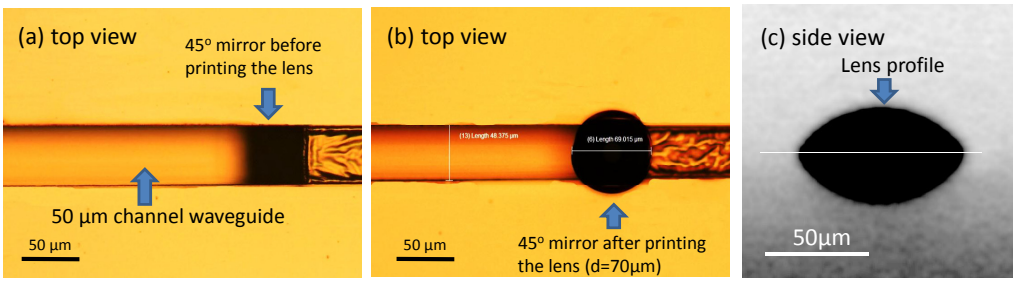

Fig. 4. (a) top view of embedded mirror before printing micro-lens (b) top view of embedded mirror after printing micro-lens with d = 70µm. (c) the lens profile taken by contact angle goniometer.

4. Optical Loss evaluation

4.1 Testing setup

Schematics of the board-to-board interconnect using the 45 degree mirrors are shown in Fig. 5. In the first experimental setup, shown in Fig. 5(a), a VCSEL (850 nm) is coupled to a 4.5 cm polymer intra-board channel waveguide through a 45 degree mirror. Another 45 degree mirror is used to couple light out of the waveguide. A PD placed on a separate board converts the optical signal into an electrical signal. In the second experiment setup, shown in Fig. 5(b), two identical waveguides (each 4.5 cm long) on separate boards with adjustable separation *d* are used to couple light from a VCSEL on one board to a PD on the other board through using four 45 degree mirrors. We also compare cases with and without micro-lenses. Figure 5 also shows the visible light spot at the output end of 1st board and 2nd board in the second experimental setup during the pre-alignment step.

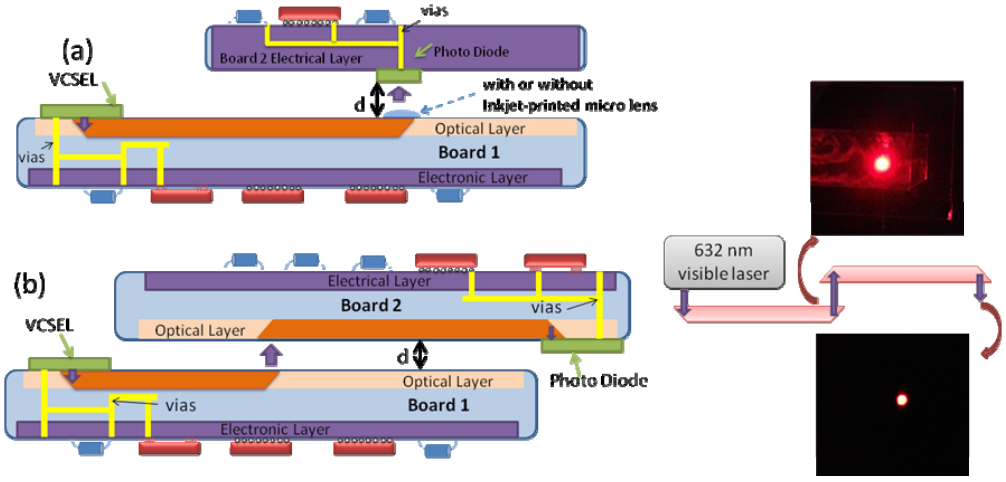

Fig. 5. Board-to-board experimental setup showing, (a) one waveguide with two 45 degree mirrors, (b) two waveguides with four 45 degree mirrors. Visible spots show the output after 2 mirrors and 4 mirrors. They are used for pre-alignment of two boards (632 nm visible laser as input, only for pre-alignment)

4.2 Optical loss evaluation

Figure 6 shows the variation of the measured optical power from the PD for 850nm wavelength as a function of the separation between the boards. The total optical loss is composed of the free space propagation loss and the insertion loss, which is determined by the coupling method and the propagation loss of the polymer waveguide. It can be seen from

#176924 - $15.00 USD Received 26 Sep 2012; revised 14 Dec 2012; accepted 15 Dec 2012; published 2 Jan 2013
(C) 2013 OSA

Fig. 6(a), for $d = 0$ (where the free space propagation loss is zero), that the measured insertion loss (without a micro-lens) is 4.586 dB. We have measured the propagation loss and scattering loss for the WIR polymer waveguides fabricated using molding method, and the loss was found to be 0.18dB/cm [41]. Therefore, each 45 mirror coupler contributes 1.888 dB loss to the optical path total loss, which corresponds to 64.86% coupling efficiency. Due to the divergence of the light coupled out of the waveguide by the 45 degree mirror, the total optical loss increases with increasing d. The divergence angle of the out-coupled beam can be reduced when a micro-lens is inserted in the optical path. Figure 6 shows 1.5 dB improvement at shorter separation (1-2 mm) and 3.7 dB improvement at larger separation (4 mm).

Furthermore, the free space coupling loss due to the beam divergence can also be extracted from the total insertion loss, as shown in Fig. 6(b). For comparison, the loss versus distance result from a previous report that utilized relatively larger lenses (240 um in diameter) mounted on both the output and input ends [9] is also plotted. The minimum loss on the results from [9] occurs at a free space propagation distance corresponding to the confocal length of the two lens system.

For the second experiment, the total insertion loss in 12 dB at $d = 1$ mm. The difference between the total insertion loss values from the two experiments remains about 4.4~4.8 dB (average = 4.528 dB) regardless of d as long as it is within 3mm. By subtracting the propagation loss (0.18 dB/cm) from all the waveguides in the second experiment, we estimate the coupling efficiency of each of the extra 45 degree mirrors in the second experiment to be 65.22%, which is very similar to the mirror coupling efficiency of the 1st board. Since the two channels are molded with the same nickel hard mold, it further confirms the process stability for such molding fabrication process.

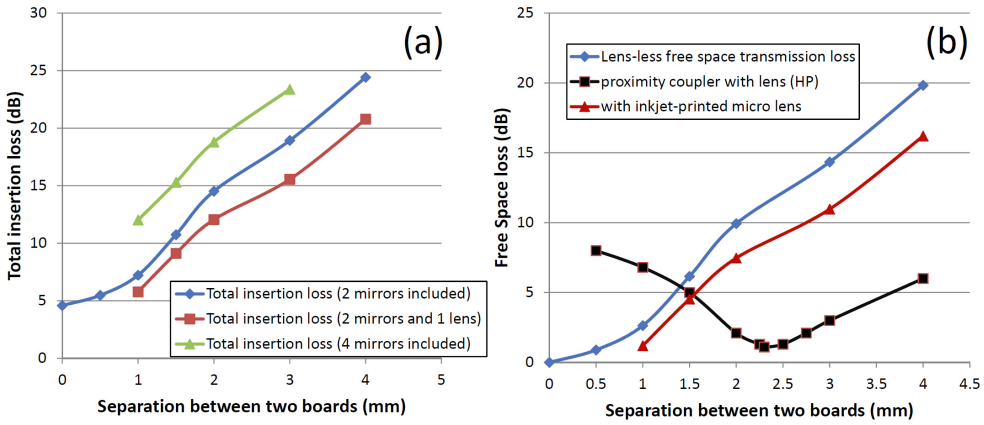

Fig. 6. (a) Total insertion loss with the separation between two boards, when 2 mirrors, 2 mirrors w/lens and 4 mirrors are included. (b) transmission loss in free space when using 45 degree coupler with/without lens and proximity coupler with lens from [9]

5. High speed communication

Beside loss evaluation, we also conducted high-speed test on the samples using the setup shown in Fig. 5(a). Light from VCSEL is directly modulated at RF frequencies ranging from 1GHz to10GHz with random signal level of ± 0.3V using Agilent ParBERT 81250 system. The separation between the input and the output boards is varied as before. The Q factors measured at $d = 0$, $d = 1$ mm and $d = 2$ mm, with and without the inkjet-printed micro-lens, as shown in Fig. 7(a). The corresponding Bit Error Rate (BER) data is shown in Fig. 7(b). The Q factor decreased quickly for $d = 2$ mm, indicating a high loss and large divergence of the beam in free space. In modern optical networks, data communication with a BER<10^{-9} is considered "error-free" [50, 51]. Without a micro-lens, at $d = 2$ mm separation case, only data

#176924 - $15.00 USD Received 26 Sep 2012; revised 14 Dec 2012; accepted 15 Dec 2012; published 2 Jan 2013
(C) 2013 OSA

rate below 3 Gbps can be transmitted error-free. On the other hand, micro-lenses increase the error-free data transmission to 7 Gbps. The eye diagrams at selected points are shown in Fig. 8, which show the improvement of the signal quality by the micro-lens.

It should be noted that using precisely positioned external lenses [38, 39] can help realize large separation coupling. However the results from Fig. 6 show the integrated ink-jet printed micro-lens can be used as part of the proximity coupler for efficient transmission over short distances (<3mm).

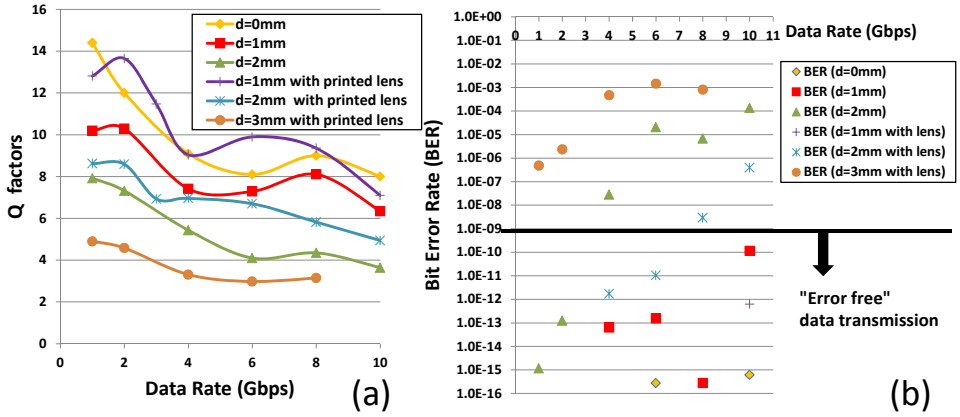

Fig. 7. (a) Q factors with different data rate, at different separations. Two mirror couplers are included in optical path. (b) Bit Error Rate distribution (BER) with data rate at different separations with/without inkjet-printed lens.

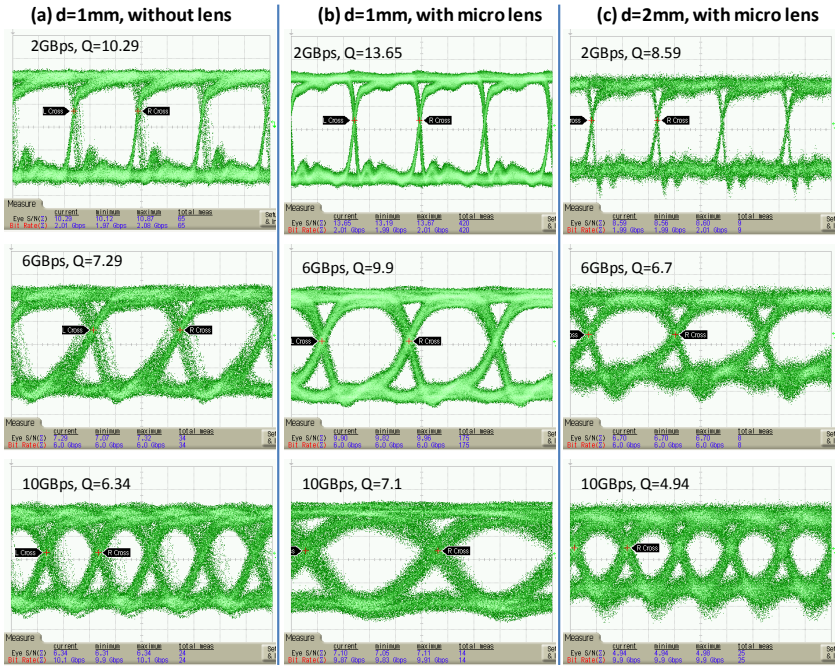

Fig. 8. Eye diagrams at selected data rate (2Gbps, 6Gbps and 10Gbps): (a) 1 mm separation with 2 mirrors; (b) 1 mm separation with 2 mirrors and 1 lens; (c) 2 mm separation with 2 mirrors and 1 lens.

#176924 - $15.00 USD Received 26 Sep 2012; revised 14 Dec 2012; accepted 15 Dec 2012; published 2 Jan 2013
(C) 2013 OSA

6. Conclusions

We presented intra- and inter-board optical interconnects using 45 degree mirror couplers and inkjet-printed micro-lens. The molding method using a low-cost electroplating technique was described and applied for optical layer fabrication. Micro-lenses (70 μm in diameter) were fabricated using an inkjet-printer. Each 45 degree mirror was shown to contribute about 1.88 dB loss (65% in coupling efficiency) to the total optical loss. The molded intra-board polymer waveguides gave 0.18 dB/cm loss. When propagating in free space without a lens, 2 mm separation resulted 9.9 dB loss, which was reduced to 7.5 dB when a micro-lens was inserted in the path using inkjet printing. At this separation, the maximum error free data rate ($BER<10^{-9}$) was measured to be 3.5Gbps and 7.5Gbps, with and without the micro-lens, respectively. At 10Gbps with micro-lens presented, 1mm and 2mm separation yielded BERs of 6.2×10^{-13} and 3.9×10^{-7}, respectively. We expect that reducing the surface roughness and angle variation of the 45 degree mirror will further improve the coupling efficiency. Also printing micro-lenses on both the input 45 degree mirror and the PD or the receiving 45 degree mirror in a confocal setup will significantly reduce the free-space propagation loss. Furthermore, the profile control of ink-jet printed micro-lens needs to be optimized in order to further increase the coupling efficiency. To achieve an optimized lens profile, lens material properties and substrate surface energy should be carefully studied. To the best of our knowledge, this is the first report of free-space coupling between waveguides on separate boards.

Acknowledgments

This work was supported in part by the National Science Foundation. The fabrication and characterization facilities at MRC of the University of Texas are supported through NNIN program.

#176924 - $15.00 USD Received 26 Sep 2012; revised 14 Dec 2012; accepted 15 Dec 2012; published 2 Jan 2013
(C) 2013 OSA